Bull. Mater. Sci., Vol. 40, No. 1, February 2017, pp. 213–222. © Indian Academy of Sciences.
DOI 10.1007/s12034-017-1358-4

Improved covalent functionalization of multi-walled carbon nanotubes using ascorbic acid for poly(amide–imide) composites having dopamine linkages

SHADPOUR MALLAKPOUR[1,2,3,*] and AMIN ZADEHNAZARI[1]

[1]Organic Polymer Chemistry Research Laboratory, Department of Chemistry, Isfahan University of Technology, Isfahan 84156-83111, I. R. Iran
[2]Nanotechnology and Advanced Materials Institute, Isfahan University of Technology, Isfahan 84156-83111, I. R. Iran
[3]Center of Excellence in Sensors and Green Chemistry, Department of Chemistry, Isfahan University of Technology, Isfahan 84156-83111, I. R. Iran

MS received 1 November 2015; accepted 20 June 2016

Abstract. **Ascorbic acid has been covalently linked to multi-walled carbon nanotubes (MWCNTs). The structures of the functionalized MWCNTs were characterized with Fourier-transform infrared spectroscopy. Thermogravimetric analysis results also demonstrated the presence of organic portions of the functionalized MWCNTs. Polymer composites based on a nanostructured poly(amide–imide) (PAI) were fabricated by an *ex situ* technique with 5, 10 and 15% loading by weight. Composite films were made by the solvent casting method. The thermal stability of the composites increased with even a small amount of modified MWCNT added. Tensile tests were conducted and depicted an increase in the elastic modulus with increasing MWCNTs content. X-ray diffraction study of the composites also indicated that the composites incorporated MWCNTs in the polymer chain.**

Keywords. **Multi-walled carbon nanotube; ascorbic acid; mechanical properties; thermal stability; transmission electron microscopy.**

1. Introduction

Carbon nanotubes (CNTs) play a fundamental role in the rapidly developing field of nanoscience and nanotechnology because of their unique properties and high potential for applications [1]. The amazing mechanical and electronic properties of the nanotubes stem from their one-dimensional (1D) structure and the graphite-like arrangement of the carbon atoms in the shells. Thus, the CNTs have high Young's modulus and tensile strength, which makes them preferable for composite materials with improved mechanical properties [2]. The composite industry faces competition from other countries doing similar research. CNT composites have the potential for becoming 'supermaterials'. If the unique properties of CNTs could be utilized in composites, we could have materials that are stronger, stiffer, more thermally conductive and more electrically conductive than anything that is used today [3,4]. In addition, they would be light and ductile. As of now, CNT composites are used only to reinforce materials, which accounts for a 10–30% increase in the materials' performance [5]. This is because the current knowledge and developments in the CNT composite industry have not attained the point where companies are able to use CNT properties to their full potential. Once CNT composites are better understood, it is likely that average consumers will see them in things they use everyday. CNT composites are already used in sporting equipment, auto parts and plastics, just to name a few examples [6–8]. Due to the above-mentioned properties, CNTs are promising reinforcing fillers for polymers too. However, commercial application of CNTs by the polymer industry has been limited so far because they are difficult to disperse in polymer matrices. Various methods of CNT chemical modification have been proved quite successful in introducing functional moieties that contribute to better nanotube dispersion, and eventually to efficient thermodynamic wetting of nanotubes with polymer matrices [9–11]. Modification methods of CNTs can be divided into two main categories based on the type of bonding to the nanotube surface. Non-covalent modification means the physical adsorption or wrapping of polymers to the surface of CNTs. The graphitic walls of CNTs provide the possibility for π-stacking interactions with conjugated polymers as well as with polymers containing heteroatoms possessing at least one free electron pair [12–14]. On the other hand, grafting of the polymer chains to the CNTs corresponds to establishing strong chemical bonds between the nanotubes and the polymer. In a subsequent reaction, the polymer chain is attached to the surface of nanotubes by addition reactions. A disadvantage of this method is that the grafted polymer content is

*Author for correspondence (mallak@cc.iut.ac.ir, mallakpour84@alumni.ufl.edu, mallak777@yahoo.com)

limited because of the relatively low reactivity and high steric hindrance of macromolecules [15,16].

The main goal of the present work was to covalently functionalize multi-walled CNTs (MWCNTs) with vitamin C structure by employing a simple one-step methodology, which was under microwave irradiation. We looked for experimental evidences of functionalization in the CNTs by using various techniques. Then, the functionalized MWCNTs were used for the preparation of poly(amide–imide) (PAI)-based composites at different MWCNTs loads. A simple sonication-assisted solution blending process for fabricating composites and a casting method for the preparation of composite films were proposed in order to study the certain properties of the resulting composites, including thermal and tensile mechanical properties.

2. Experimental

2.1 *Materials*

Carboxylated MWCNTs synthesized by chemical vapour deposition (CVD) process (the outer diameter 8–15 nm, the inner diameter 3–5 nm, length ~50 μm, carboxyl content 2.56 wt% and purity >95 wt%), were obtained from Neutrino Co. (Iran). Dopamine hydrochloride, 3,5-dinitrobenzoylchloride, trimellitic anhydride (TMA), L-isoleucine amino acid, glacial acetic acid, propylene oxide, tetrabutylammonium bromide (TBAB) and triphenyl phosphite (TPP) were achieved commercially from Fluka Chemical Co. (Switzerland), Aldrich Chemical Co. (Milwaukee, WI) and Merck Chemical Co. (Germany). These chemicals were used as received without further purification. Propylene oxide was used as an acid scavenger. Hydrazine monohydrate and 10% palladium on activated carbon were used as obtained. N,N-dimethylformamide (DMF) ($d = 0.94\,\mathrm{g\,cm^{-3}}$ at 20°C) and N,N-dimethylacetamide (DMAc) ($d = 0.94\,\mathrm{g\,cm^{-3}}$ at 20°C) as solvents were distilled over barium oxide under reduced pressure before use.

2.2 *Instruments and characterization methods*

The equipment used for the functionalization of MWCNTs and synthesis of the polymer was a Samsung microwave oven (2450 MHz, 900 W) (Seoul, South Korea). Melting points of the monomers were measured on a melting-point equipment (Gallenhamp, Cambridge, United Kingdom) without correction. ^{1}H nuclear magnetic resonance (NMR) spectrum was recorded on a Bruker (Rheinstetten, Germany) Avance 500 instrument at room temperature in dimethylsulphoxide-d_6 (DMSO-d_6). Multiplicities of proton resonance were designated as singlet (s), doublet (d), triplet (t) and multiplet (m). The chemical shifts were reported in ppm. Fourier transform infrared (FT-IR) spectra of the samples were recorded with a Jasco-680 (Tokyo, Japan) spectrometer [taken in potassium bromide (KBr)] at a resolution of $4\,\mathrm{cm^{-1}}$. They were scanned in the wavenumber range of 400–4000 $\mathrm{cm^{-1}}$. Band intensities were assigned as weak (w), medium (m), strong (s) and broad (br). Vibration bands were reported as wavenumber ($\mathrm{cm^{-1}}$). Elemental analysis was run on an Elementar Analysensysteme GmbH (Hanau, Germany). Inherent viscosity was measured using a Cannon Fenske Routine Viscometer (Mainz, Germany) at the concentration of 0.5 g $\mathrm{dl^{-1}}$ in DMF at 25°C. Optical specific rotation was measured at the concentration of 0.5 g $\mathrm{dl^{-1}}$ in DMF at 25°C using a quartz cell (1.0 cm) with a Jasco Polarimeter (JASCO Co., Ltd, Tokyo, Japan). Thermal stability of MWCNTs, PAI and MWCNT-AS/PAI nanocomposites was evaluated by recording thermogravimetric analysis (TGA) traces (STA503 TGA, Bahr-Thermoanalyse GmbH, Hüllhorst, Germany) in nitrogen atmosphere (flow rate $60\,\mathrm{cm^3\,min^{-1}}$). A heating rate of $10°\mathrm{C\,min^{-1}}$ and a sample size of 10 ± 2 mg were used in each experiment. The X-ray diffraction (XRD) analyses were carried out on a Bruker, D8AVANCE (Rheinstetten, Germany) diffractometer using a Cu Kα radiation source. The samples were scanned at a rate of $0.05°\,\mathrm{min^{-1}}$ from 10° to 80° of 2θ. The morphology of the MWCNTs and dispersion morphology of the MWCNTs-AS on the PAI matrix were observed using field emission scanning electron microscopy (FE-SEM). The images were taken at 15 kV using a HITACHI S-4160 instrument (Tokyo, Japan). Transmission electron microscopy (TEM) images were taken with a Philips CM 120 microscope (Netherlands) with an accelerating voltage of 100 kV. For TEM studies, ultra-thin sections (30–80 nm) of the composites were prepared using a Leica Ultramicrotome. Tensile testing was performed at room temperature on a Testometric Universal Testing Machine M350/500 (Mainz, Germany), according to ASTM D 882 (standards). Tests were carried out with a cross-head speed of $12.5\,\mathrm{mm\,min^{-1}}$ until reaching a deformation of 20%, and then at a speed of $50\,\mathrm{mm\,min^{-1}}$ at break. The dimensions of the test specimens were $35 \times 2 \times 0.04\,\mathrm{mm^3}$. Property values reported here represent an average of the results for tests run on at least five specimens. Tensile strength, tensile modulus and strain were obtained from these measurements. The composites were prepared using a MISONIX ultrasonic XL-2000 SERIES (Raleigh, North Carolina, USA). Ultrasonic irradiation was performed with the probe of the ultrasonic horn being immersed directly into the mixture solution system with the frequency of 2.25×10^4 Hz and the power of 100 W.

2.3 *Monomer synthesis*

The synthesis of N-trimellitylimido-L-isoleucine (3) has been previously described (figure 1) [17].

3,5-Diamino-N-(3,4-dihydroxyphenethyl)benzamide (4) as a diamine monomer was also prepared according to our reported procedure [18].

2.4 *Functionalization of MWCNT*

A schematic representation of functionalization of MWCNTs with ascorbic acid is shown in figure 2, according to our previous work [19].

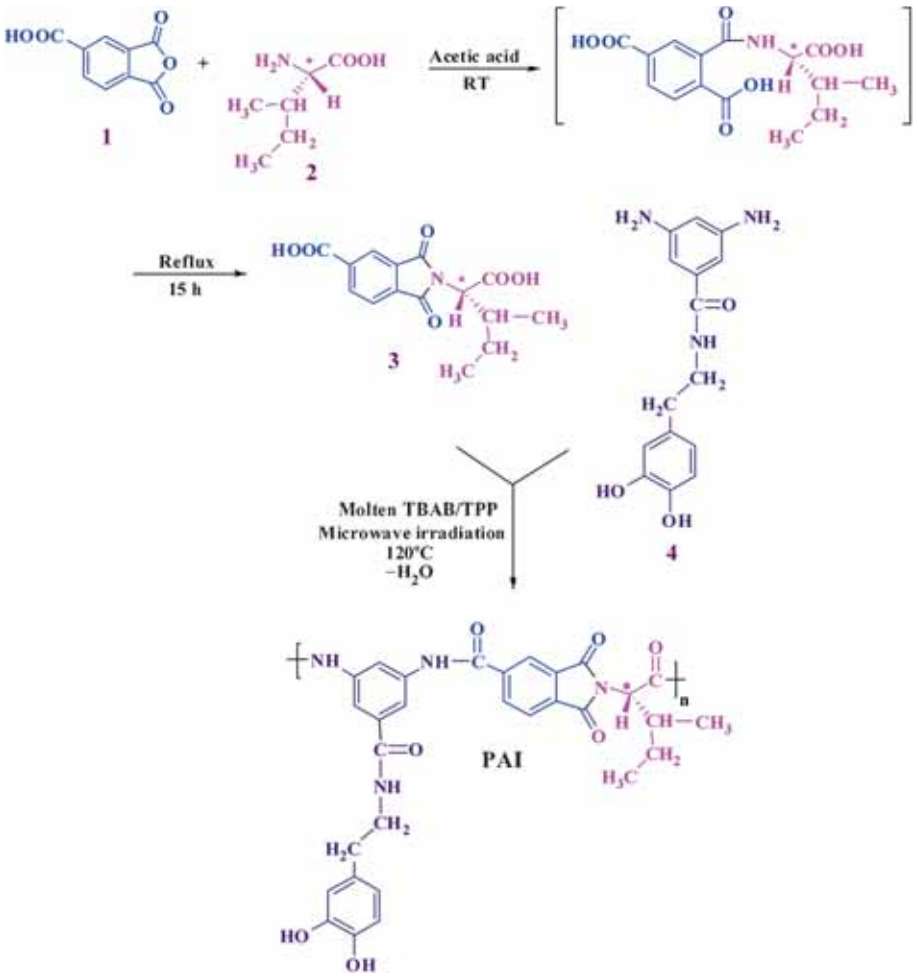

Figure 1. Synthesis strategy for diacid monomer 3 and PAI.

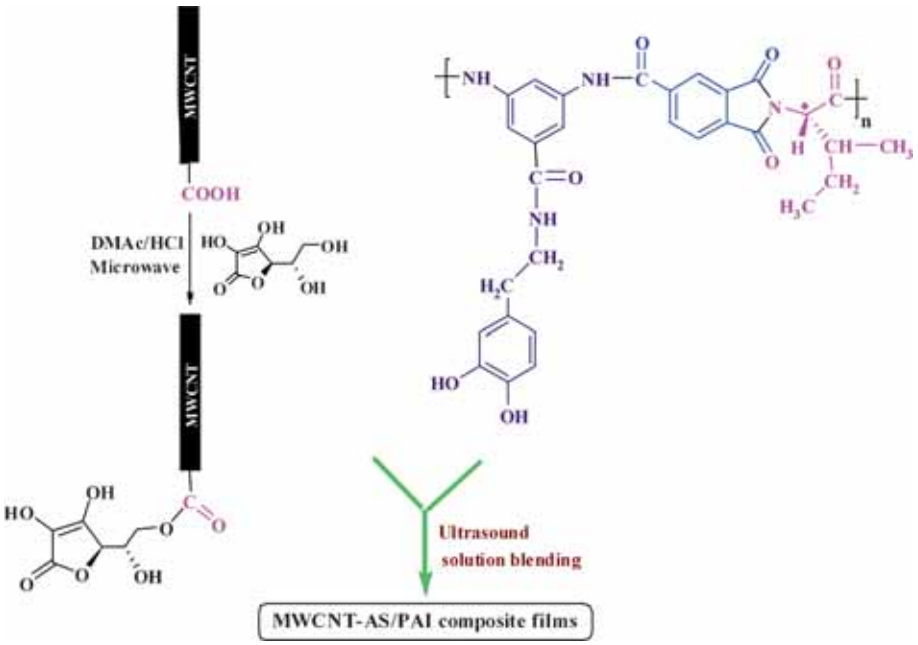

Figure 2. Schematic representation of the attachment of vitamin C with MWCNTs and preparation of their PAI-based composites.

2.5 *Polymer synthesis*

A quantity of 0.10 g (3.27×10^{-4} mol) of diacid monomer 3, 0.094 g (3.27×10^{-4} mol) of diamine 7 and 0.42 g of TBAB (1.31×10^{-3} mol) were placed in a porcelain dish and ground completely for 5 min; then, 0.34 ml (1.31×10^{-3} mol) of TPP was added and the mixture was ground for 3 min. The reaction mixture was irradiated in the microwave oven for 240 s at 100% of power level (900 W) (the temperature of the reaction was 12°C). The resulting viscous solution was poured into 30 ml of methanol, filtered and dried at 80°C for 6 h under vacuum to give 0.13 g (94%) of yellow powder PAI. The optical specific rotation was measured ($[\alpha]^{25}_{Na,589} = -35.1°$) at a concentration of 0.5 g dl^{-1} in DMF at 25°C. The inherent viscosity was also measured ($\eta_{inh} = 0.48$ dl g^{-1}) under the same conditions.

FT-IR (KBr, cm^{-1}): 3416 (m, br, NH and OH stretching), 3114 (w, C–H aromatic), 2963 (w, C–H aliphatic), 2927 (w, C–H aliphatic), 1776 (m, C=O imide, asymmetric stretching), 1717 (s, C=O imide, symmetric stretching), 1647 (m, C=O amide, stertching), 1599 (s), 1550 (m), 1446 (s), 1376 (m, C–N–C axial stretching), 1198 (m, C–N–C transverse stretching), 1073 (m), 865 (m), 766 (m), 725 (s, C–N–C out-of-plane bending), 683 (w). ^{1}H NMR (400 MHz, DMSO-d_6, ppm): 0.91 (t, 3H, CH_3, distorted), 1.29 (d, 3H, CH_3, $J = 7.20$ Hz), 1.50 (m, 2H, CH_2), 2.59 (m, 1H, CH), 2.87 (t, 2H, CH_2, distorted), 3.15 (t, 2H, CH_2, distorted), 4.63–4.65 (d, 1H, CH, $J = 8.40$ Hz), 6.45–6.47 (d, 1H, Ar–H, $J = 8.40$ Hz), 6.61–6.63 (d, 1H, Ar–H, distorted), 7.66 (s, 1H, Ar–H), 7.71 (s, 1H, Ar–H), 7.94 (s, 1H, Ar–H), 8.00 (s, 1H, Ar–H), 8.10 (d, 1H, Ar–H, distorted), 8.46 (s, 1H, Ar–H), 8.51–8.53 (d, 1H, Ar–H, distorted), 8.76 (s, 1H, NH), 10.15 (s, 1H, OH), 10.23 (s, 1H, OH), 10.78 (s, 1H, NH), 10.85 (s, 1H, NH).

Elemental analysis calculated for $(C_{30}H_{28}N_4O_7)_n$: C, 64.74%; H, 5.07%; N, 10.07%. Found: C, 64.35%; H, 4.96%; N, 10.29%.

2.6 *Preparation of the MWCNT-AS/PAI composite films*

PAI powder was dissolved and MWCNTs-AS was separately dispersed in DMAc with stirring for 1 day at 30–40°C. Then, the solutions were mixed to attain the desired weight percentages of MWCNTs-AS from 5 to 15 wt%. The MWCNT-AS/PAI mixture was stirred for 1 day at 30–40°C and then ultrasonicated in a water bath for 1 h. By casting this suspension on to a clean glass or stainless slide, evaporating DMAc at 60°C for 1 day, and then at 160°C for 8 h the composites were obtained.

3. Results and discussion

3.1 *Polymer synthesis*

The dopamine containing PAI was synthesized according to the synthesis route shown in figure 1. Condensation of the monomers 3 and 4 in molten TBAB and in the presence of TPP as catalyst under microwave irradiation was applied for the synthesis of PAI. TBAB is soluble in the polar solvents such as water and methanol, which allowed the complete isolation of obtained polymer. The optimized condition for irradiation was 100% of power level, 120°C for 240 s. The PAI was obtained as yellow powder with good yield, 94%, after extraction with refluxing methanol for 24 h to remove low fraction oligomers, and its inherent viscosity was 0.48 dl g^{-1}. Because of its nature TBAB has very low vapour pressure and is characterized by the absence of strong acid or alkaline properties; therefore, the risk of polymer's hydrolysis at the isolation along with the necessity of its thorough purification is no longer relevant. The polymer structure was confirmed by elemental analysis, FT-IR and ^{1}H-NMR spectroscopic techniques [20].

3.2 *Composite films preparation*

MWCNT-AS composite films were produced by solution blending; 5, 10 and 15 wt% of MWCNT-AS with PAI powder were mixed in DMAc with ultrasonic assistance. The reaction pathway is shown in figure 2. According to previous literature, the aforementioned weight percents were selected [21–25]. The introduction of several functional groups as well as dopamine and amino acid bulky substituents resulted in increased chain packing distances and decreased intermolecular interactions, leading to better interaction of the PAI chains with MWCNTs-AS and better dispersion of MWCNTs-AS in the PAI matrix. These interactions are illustrated in figure 3.

3.3 *Characterization of MWCNTs and the composites*

3.3a *FT-IR and ^{1}H NMR*: The spectral analysis data indicated the successful incorporation of ascorbic acid onto MWCNT surfaces through esterification reaction. Figure 4 shows FT-IR spectra of the MWCNT-COOH and the MWCNT-AS. The organic moieties of MWCNT-AS were characterized with the absorptions of the –OH groups at 3425 cm^{-1}, –CH groups at 2926 cm^{-1}, –COO– groups at 1735 cm^{-1} and –C–O– groups at 1118 cm^{-1} in its FT-IR spectrum. The spectrum of a carboxylated MWCNTs/KBr pellet showed a strong, broad absorption band centred at 3433 cm^{-1}, which could be related to the stretching vibration of O–H bands of carboxylic acid moieties from the surface of MWCNTs. The small peak around 2923 cm^{-1} was ascribed to aliphatic sp^3 C–H of MWCNTs [26]. Strong band of absorption characteristic for the acid linkage appeared at 1629 cm^{-1} assigned to C=O stretching vibration. The structure of PAI was also confirmed by using FT-IR spectroscopy. Strong absorption bands were observed at 1776 cm^{-1}. This can be related to the asymmetric and symmetric stretching vibrations of the imide carbonyl groups. The bands of C–N bond stretching and ring deformation appeared at 1376 and 725 cm^{-1}. Strong bands of absorption were characteristic of

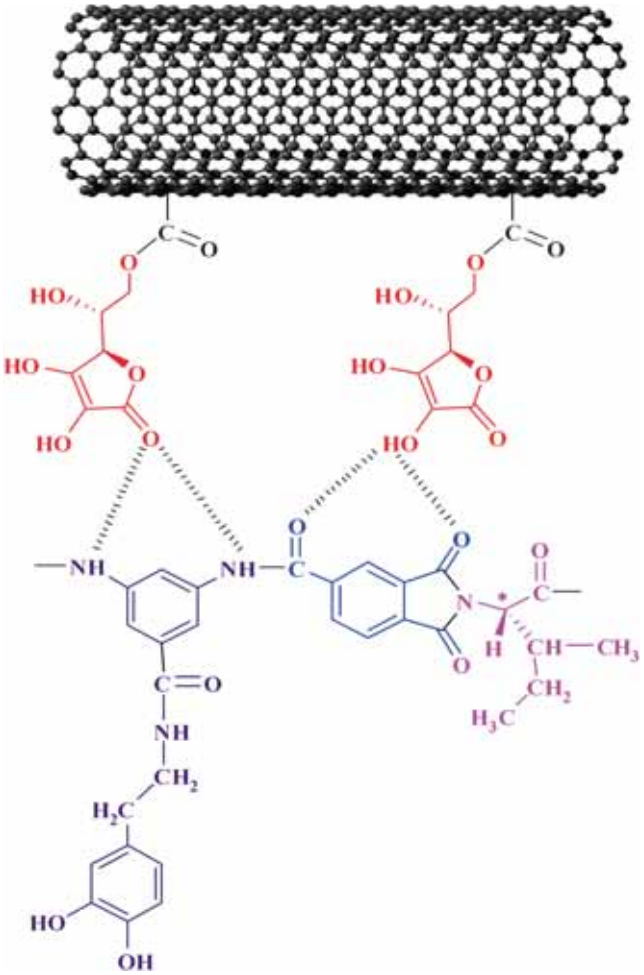

Figure 3. Interactions of H-bonding between the MWCNT-AS and the PAI chains.

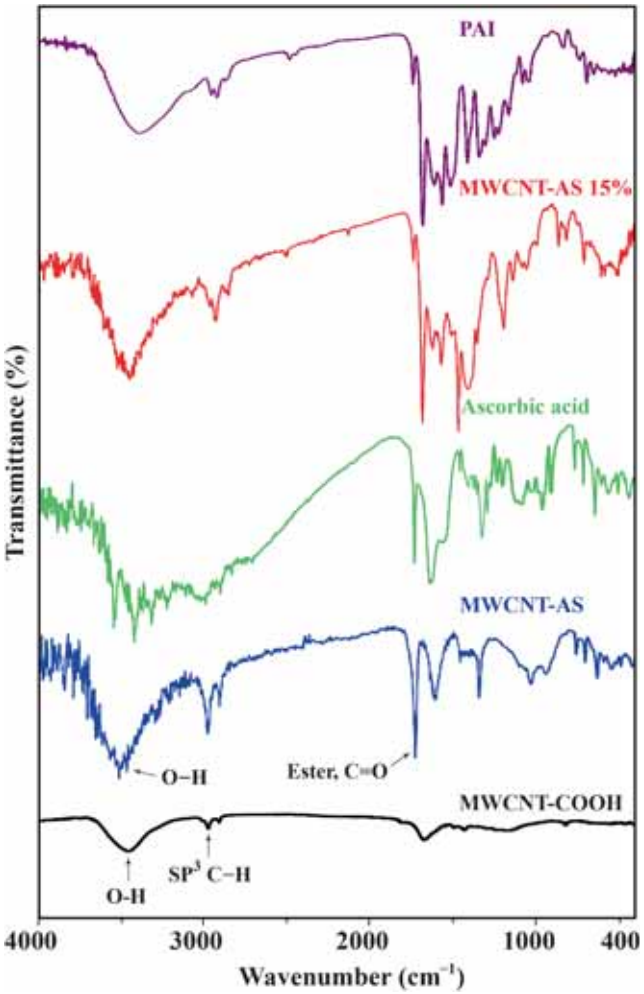

Figure 4. FT-IR spectra of MWCNT-COOH, MWCNT-AS, PAI and the composite containing 15 wt% of MWCNT-AS.

the hydroxyl groups and the newly formed amide linkage appeared at around 3416 cm^{-1}. They were assigned to O–H and N–H stretching vibrations at 1647 cm^{-1}, which can be attributed to amide C=O stretching vibration; at 1550 cm^{-1}, they were due to N–H bending vibration. The absorption band at around 3114 cm^{-1} was attributed to =CH aromatic linkage. The aliphatic C–H stretching peak also appeared at around 2963 cm^{-1} [27]. The presence of MWCNTs-AS in the polymer matrix showed very few changes in the FT-IR spectrum, presumably due to the low MWCNT-AS composition and the weak vibration signals of MWCNTs. Figure 4 shows the representative FT-IR spectrum of MWCNT-AS/PAI 15 wt%.

The structure of neat PAI was also identified by ^{1}H NMR spectroscopy. In the ^{1}H NMR spectrum of this polymer, the presence of the N–H protons of amide groups at 8.76, 10.78 and 10.85 ppm as three singlet peaks, and O–H groups at 10.15 and 10.23 ppm as two singlet peaks, indicated the presence of amide groups in the polymer's side chain as well as main chain and hydroxyl groups in the polymer's side chain. The resonance of aromatic protons appeared in the range of 6.45–8.53 ppm. The proton of the chiral centre appeared as doublet at 4.63–4.65 ppm. The elemental analysis results were also in good conformity with calculated percentages of carbon, hydrogen and nitrogen contents in the polymer-repeating units, indicating that the expected compound was obtained.

3.3b *Crystallization behaviour*: The crystallization behaviours and crystalline structure were investigated using XRD. In the case of MWCNTs, two peaks appeared at $2\theta = 26°$ and 44°, which are typically associated with diffraction metal impurities [$2\theta = 26°$ corresponds to the (002) diffraction plane of the impurity graphite and $2\theta = 44°$ to α-Fe (110) and/or Ni (111) diffractions] [28]. MWCNTs-AS showed very few changes in the XRD pattern. For the pristine PAI, an obvious broad peak centred at $2\theta = 20°$ indicates that the PAI polymer is amorphous. For the MWCNT content higher than 10 wt%, the composites exhibit peaks of PAI and MWCNTs, as show in figure 5. The intensity of the peaks assigned to the MWCNTs in the composites increases with an increasing proportion of MWCNTs.

3.3c *FE-SEM*: The typical microstructure of the unmodified and modified MWCNTs investigated by FE-SEM is presented in figure 6. As can be seen, the MWCNTs-COOH surface is about flat, but the MWCNT-AS surface is rough. The morphologies of PAI and MWCNT/PAI composites are shown in figure 7. The PAI copolymer showed a corn-like morphology. The CNTs in the PAI matrix were observed as individual tubes.

3.3d *TEM*: The TEM images of the MWCNT-AS are presented in figure 8 (top). Compared with the carboxylated MWCNTs (figure 8, bottom), MWCNTs-AS are present in a form of smaller bundles and no longer have a smooth surface, which has been attributed to the groups attached to the nanotube wall. Figure 9 is the TEM observation of the dispersion of the modified MWCNTs in the PAI matrix (mass fraction of MWCNTs is 10 wt%). It can be seen that the MWCNTs were almost attached to the polymeric particles, resulting from the increased polarity by the functional groups formed on the surfaces of MWCNTs as well as carbonyl groups in the PAI structure.

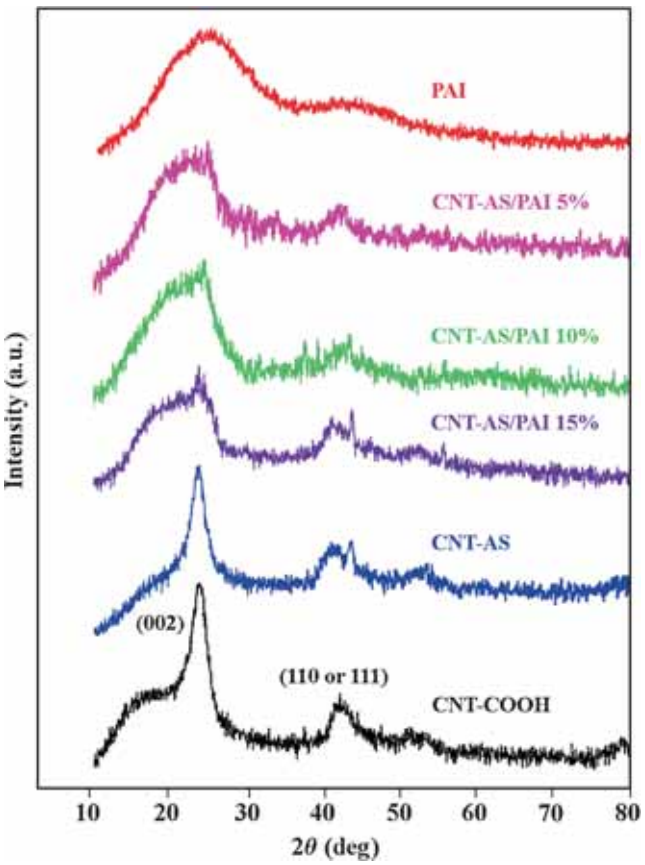

Figure 5. XRD pattern for CNT-COOH, CNT-AS and CNT-AS/PAI composites samples with different CNT-AS contents.

3.3e *Mechanical properties*: The tensile stress–strain curve is a tool to provide data on toughness (area under the curve), ultimate tensile strength, ultimate elongation at break and Young's modulus. Figure 10 presents the stress–strain curves for PAI loaded with 0, 5, 10 and 15 wt% of MWCNTs-AS. The mechanical properties calculated from the stress–strain curves are shown in table 1. The results show that Young's modulus and tensile strength increase steadily with the addition of the MWCNTs-AS. From the table, we can see the noticeable trend of tensile strength of specimens increased on increasing the MWCNT content, while the tensile elongation and the area under the curve, which is used to measure the fracture energy or static toughness, decreased. The reinforcing efficiency of MWCNT-AS is defined as the normalized mechanical properties of the composites with respect to those of pure PAI. The general tendency for improvement in the stress level is increased by the addition of CNTs, which play the role of reinforcement. Another reason for the enhancements in the tensile modulus of composites is the strong interaction between the PAI matrix and MWCNTs-AS via formation of hydrogen and non-covalent bonding.

3.3f *Thermal properties*: The thermal properties results of PAI, nanocomposites and the MWCNTs are given in tables 2 and 3. Besides, figure 11 shows TGA curves of the samples. The curve of pristine CNT showed a small mass loss in a temperature range of 0–550°C. The weight loss of MWCNT-AS resulted from the decomposition of the functionalized organic moieties attached to the surface of

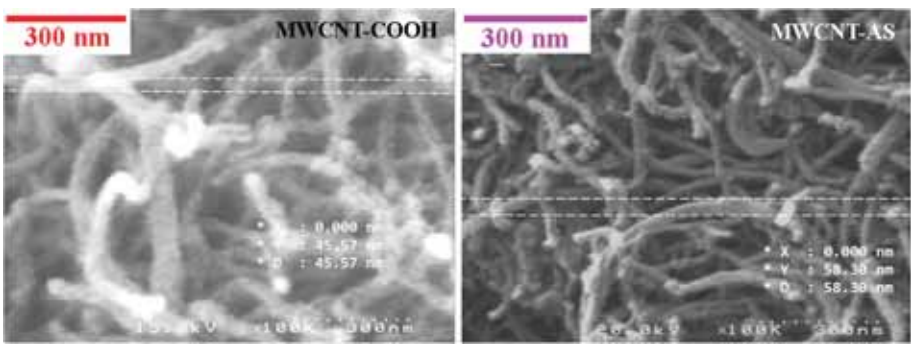

Figure 6. FE-SEM micrograph of MWCNT-COOH and MWCNT-AS.

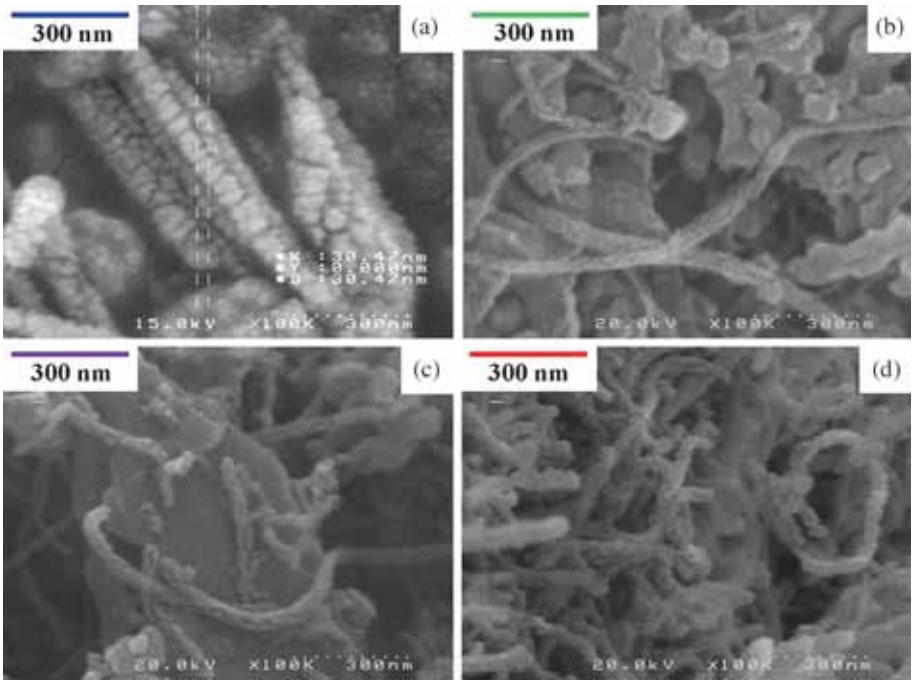

Figure 7. FE-SEM micrographs of (**a**) neat PAI and the composites containing (**b**) 5 wt%, (**c**) 10 wt% and (**d**) 15 wt% of MWCNTs-AS.

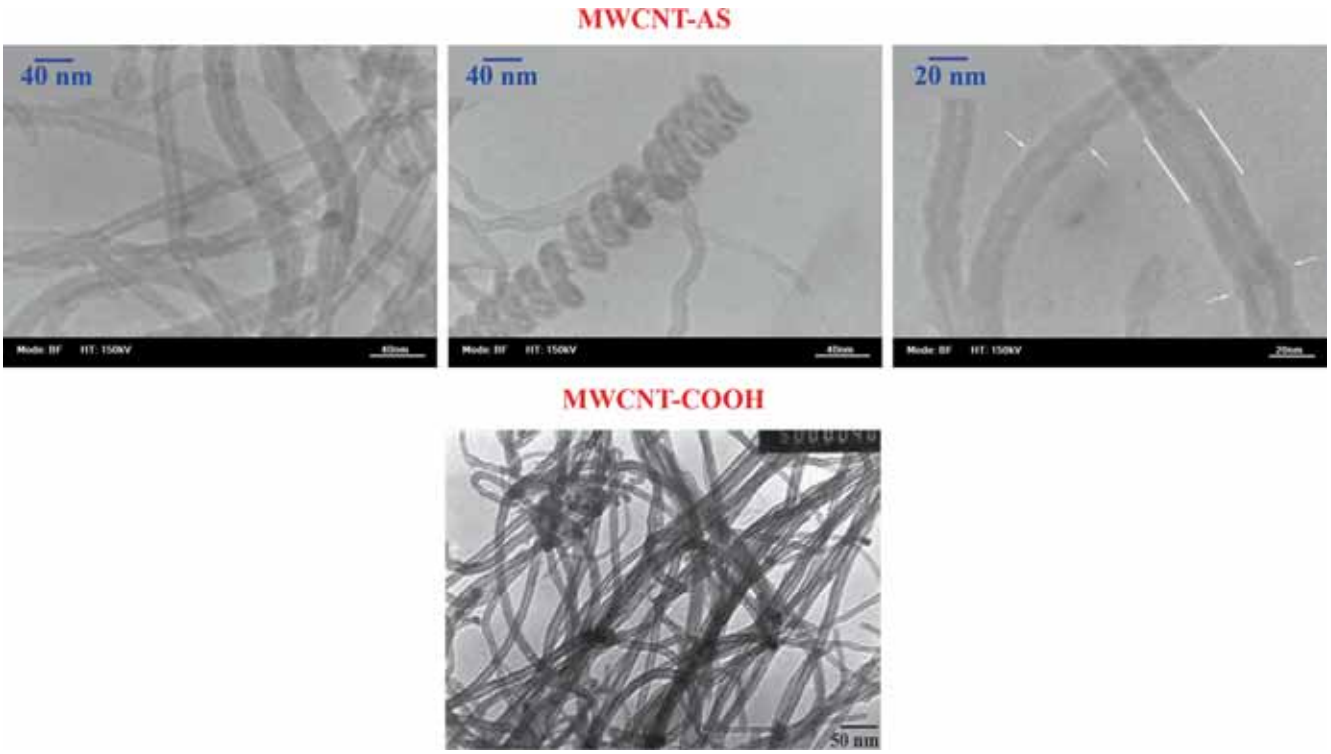

Figure 8. TEM images of MWCNT-AS at different magnifications.

MWCNTs. TGA data of the pristine and the purified MWCNTs suggested that the MWCNTs were able to withstand oxidation temperatures up to 700°C. This could be due to the incorporation of carboxyl groups in the defective sites and tips. The initial decomposing temperature of the MWCNT-COOH was 550°C, indicating that the MWCNTs-COOH was thermally stable up to this temperature, as shown in table 2. The modified MWCNTs decomposed slowly from

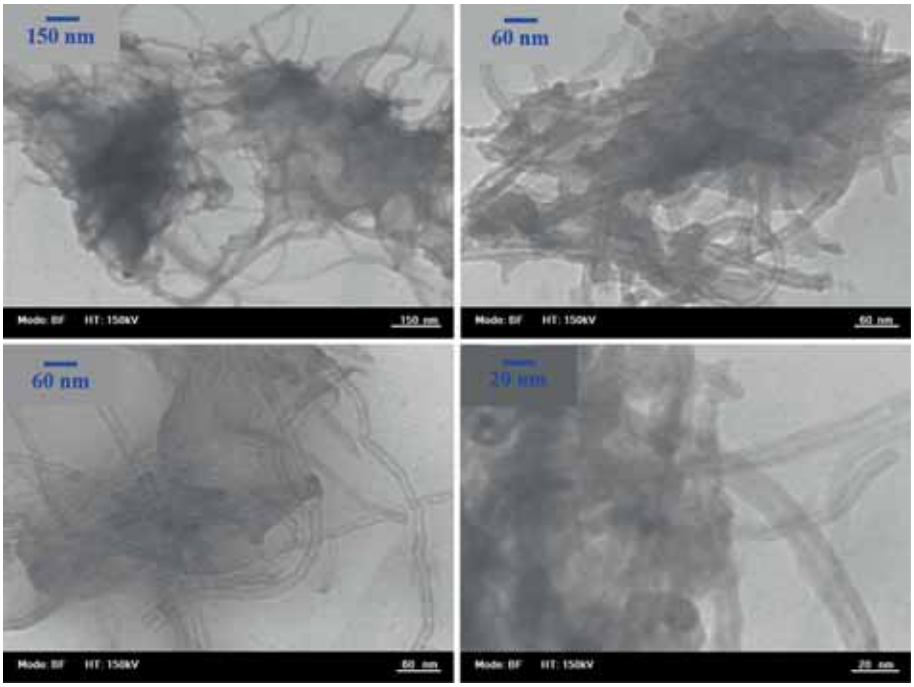

Figure 9. TEM images of MWCNTs-AS/PAI composites containing 10 wt% of MWCNT-AS.

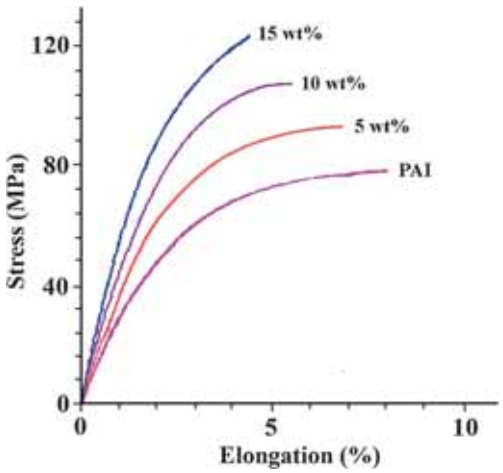

Figure 10. Tensile stress–strain curves of MWCNTs-AS/PAI composites for concentrations ranging from 0 to 15% MWCNTs-AS by weight.

220°C because of the losing organic groups on the surface of MWCNTs. By comparing the MWCNTs-AS with MWCNTs-COOH, it can be concluded that the thermal stability of MWCNTs-COOH was destroyed upon functionalization with ascorbic acid. The thermal behaviour data for the PAI and the composites are summarized in table 3. The thermal stability of the MWCNT/PAI composites increased linearly with increasing MWCNT-AS content. This could be related to the higher heat transfer of CNTs, which facilitated heat dissipation within the composites, hence preventing the accumulation of heat at certain points for degradation [29]. The end temperature of decomposition was also retarded with increasing MWCNT-AS content. The weight percent remaining after major degradation at 800°C was higher for composites rather than neat PAI. This indicated that MWCNT reduced the degradation of PAI at high temperature as the effect was clearly seen in the curves. Therefore, it could be verified that a small amount of MWCNT acted as effective thermal-degradation-resistant reinforcement in the PAI matrix, increasing the thermal stability of the MWCNT/PAI composites.

The limiting oxygen index (LOI) is the minimum concentration of oxygen that will support combustion of a polymer expressed as a percentage. It can be used to evaluate the flame retardancy of the polymers. Normal atmospheric air is approximately 21% oxygen; hence a material with an LOI of less than 21% would burn easily in air. That being said, a material with LOI of greater than 21% but less than 28% would be considered 'slow burning'. A material with LOI of greater than 28% would be considered 'self-extinguishing'. A self-extinguishing material is one that would stop burning after the removal of the fire or ignition source [30].

Theoretically, two interesting relationships have been found between the LOI and the parameters of the combustion process: char yield or char residue (CR) and heat of combustion.

According to Van Krevelen [31], there is a linear relationship between LOI and CR only for halogen-free macromolecules:

$$\mathrm{LOI} = (17.5 + 0.4\mathrm{CR})/100. \quad (1)$$

This equation implies that a higher char yield will improve flame retardance. PAI and composites having 5, 10 and

Table 1. Mechanical properties from tensile testing for CNT-AS/PAI composite films.

Sample	Tensile strength (MPa)	Young's modulus (GPa)	Elongation at break (%)
PAI	79.4 ± 0.2	2.0 ± 0.1	8.1 ± 0.4
CNT-AS/PAI 5 wt%	94.1 ± 0.2	2.3 ± 0.2	6.9 ± 0.5
CNT-AS/PAI 10 wt%	108.5 ± 0.1	2.7 ± 0.3	5.6 ± 0.7
CNT-AS/PAI 15 wt%	120.2 ± 0.1	3.0 ± 0.1	4.5 ± 0.5

Table 2. Thermal stability of CNT samples obtained from TGA thermograms.[a]

Sample	T_{d5} (°C)	Weight residue at 800°C
MWCNT-COOH	550	90
MWCNT-AS	274	60

[a]Temperature at which 5% weight loss was recorded by TGA at a heating rate of 10°C min^{-1} in a nitrogen atmosphere.

Table 3. Thermal properties of PAI and the composites.[a]

MWCNT-AS content (%)	T^{a}_{d5} (°C)	T^{a}_{d10} (°C)	CR (%)[b]	LOI (%)[c]
0	326	398	45	35.5
5	335	406	48	36.7
10	380	432	52	38.3
15	426	467	58	40.7

[a]Temperature at which 5 and 10% weight loss was recorded by TGA at a heating rate of 10°C min^{-1} in a nitrogen atmosphere.
[b]Percentage weight of material left undecomposed after TGA analysis at maximum temperature of 800°C in a nitrogen atmosphere.
[c]Limiting oxygen index (LOI) evaluated from char yield at 800°C.

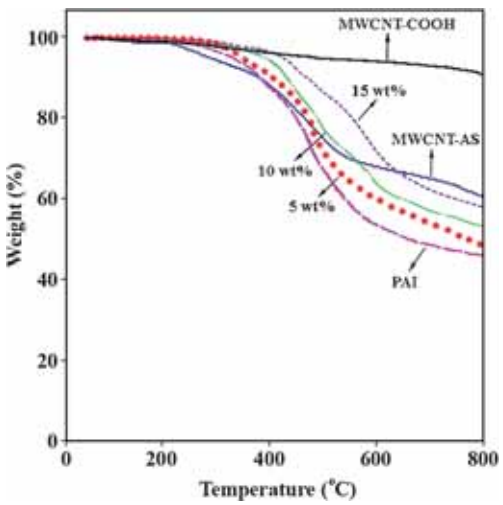

Figure 11. TGA curves of the composites with different MWCNT-AS loadings.

15 wt% MWCNTs-AS had LOI values of 35.5, 36.7, 38.3 and 40.7, respectively, as determined from their CR. On the basis of the LOI values, such materials can be categorized as self-extinguishing materials.

4. Conclusions

The ascorbic acid structures, grafted to the MWCNTs through the esterification reaction, improved the dispersal and stability of MWCNTs in a PAI matrix. MWCNTs/PAI nanocomposite thin films containing different MWCNT-AS loadings were prepared using solution blending and the ultrasonic dispersion method. Electronic microphotographs suggested that MWCNTs-AS were uniformly distributed in the PAI matrix. The effects of MWCNTs-AS content on the mechanical behaviour of thin films have been studied. Mechanical tensile tests indicated that the appropriate addition of MWCNTs into the PAI matrix can significantly improve the elastic modulus of PAI. TGA results showed that the hybrid films exhibit a good thermal stability. All the experimental results allow concluding that the functionalization process represents an effective method to graft compatibilizing agents onto the surfaces of CNTs. The high added value of this process is that it is cost-effective, ecosustainable, simple and easy to scale up.

Acknowledgements

We are grateful to the Research Affairs Division of Isfahan University of Technology (IUT), National Elite Foundation (NEF) and Center of Excellency in Sensors and Green Chemistry Research (IUT).

References

[1] Moradi O, Yari M, Zare K, Mirza B and Najafi F 2012 *Fullerenes, Nanotubes Carbon Nanostruct.* **20** 138

[2] Shokrieh M and Rafiee R 2010 *Mech. Compos. Mater.* **46** 155

[3] Behabtu N, Young C C, Tsentalovich D E, Kleinerman O, Wang X, Ma A W, Bengio E A, ter Waarbeek R F, de Jong J J and Hoogerwerf R E 2013 *Science* **339** 182

[4] Chen W-J, Li Y-L, Chiang C-L, Kuan C-F, Kuan H-C, Lin T-T and Yip M-C 2010 *J. Phys. Chem. Solids* **71** 431

[5] Saligheh O, Forouharshad M, Arasteh R, Eslami-Farsani R, Khajavi R and Roudbari B Y 2013 *J. Polym. Res.* **20** 1

[6] Brosseau C 2011 *Surf. Coat. Technol.* **206** 753

[7] Ryan K P, Cadek M, Nicolosi V, Blond D, Ruether M, Armstrong G, Swan H, Fonseca A, Nagy J B and Maser W K 2007 *Compos. Sci. Technol.* **67** 1640

[8] Kuan C-F, Chen W-J, Li Y-L, Chen C-H, Kuan H-C and Chiang C-L 2010 *J. Phys. Chem. Solids* **71** 539

[9] Oki A, Adams L, Luo Z, Osayamen E, Biney P and Khabashesku V 2008 *J. Phys. Chem. Solids* **69** 1194

[10] Bernal M M, Liras M, Verdejo R, López-Manchado M A, Quijada-Garrido I and París R 2011 *Polymer* **52** 5739

[11] Gaina C, Ursache O, Gaina V and Ionita D 2011 *Polym. Plast. Technol. Eng.* **51** 65

[12] Osazuwa O, Kontopoulou M, Xiang P, Ye Z and Docoslis A 2012 *Proc. Eng.* **42** 1543

[13] Zhang A, Tang M, Luan J and Li J 2012 *Mater. Lett.* **67** 283

[14] Mallakpour S and Zadehnazari A 2013 *Carbon* **56** 27

[15] de Freitas J N, Maubane M S, Bepete G, van Otterlo W A L, Coville N J and Nogueira A F 2013 *Synth. Met.* **176** 55

[16] Shi X, Wang J, Jiang B and Yang Y 2013 *Polymer* **54** 1167

[17] Mallakpour S, Hajipour A R and Hassan Shahmohammadi M 2003 *J. Appl. Polym. Sci.* **89** 116

[18] Mallakpour S, Hatami M, Ensafi A A and Karimi-Maleh H 2011 *Chin. Chem. Lett.* **22** 185

[19] Mallakpour S and Zadehnazari A 2014 *J. Solid State Chem.* **211** 136

[20] Mallakpour S and Zadehnazari A 2012 *Polym. Plast. Technol. Eng.* **51** 1090

[21] Mallakpour S and Zadehnazari A 2014 *Bull. Mater. Sci.* **37** 1065

[22] Mallakpour S and Zadehnazari A 2014 *Polym. Int.* **63** 1203

[23] Al-Saleh M H and Sundararaj U 2009 *Carbon* **47** 1738

[24] Peng F, Pan F, Sun H, Lu L and Jiang Z 2007 *J. Membr. Sci.* **300** 13

[25] Mohiuddin M and Hoa S 2011 *Compos. Sci. Technol.* **72** 21

[26] Lee H-J, Oh S-J, Choi J-Y, Kim J-W, Han J, Tan L-S and Baek J-B 2005 *Chem. Mater.* **17** 5057

[27] Hsiao S-H, Guo W, Lee W-F, Kung Y-C and Lee Y-J 2011 *Mater. Chem. Phys.* **130** 1086

[28] Perez-Cabero M, Rodrıguez-Ramos I and Guerrero-Ruız A 2003 *J. Catal.* **215** 305

[29] Huxtable S T, Cahill D G, Shenogin S, Xue L, Ozisik R, Barone P, Usrey M, Strano M S, Siddons G and Shim M 2003 *Nat. Mater.* **2** 731

[30] Bucsi A and Rychlý J 1992 *Polym. Degrad. Stab.* **38** 33

[31] Van Krevelen D 1975 *Polymer* **16** 615